Published in final edited form as:
J Shoulder Elbow Surg. 2014 May ; 23(5): 708–719. doi:10.1016/j.jse.2013.08.014.

Three-dimensional Humeral Morphological Alterations and Atrophy Associated with Obstetrical Brachial Plexus Palsy

Frances T. Sheehan, PhD[1], **Sylvain Brochard, MD**[1,2,3], **Abrahm J. Behnam, MS**[1,4], and **Katharine E. Alter, MD**[1,5]

[1]Functional and Applied Biomechanics Section, Rehabilitation Medicine Department, National Institutes of Health, Bethesda, MD, USA

[2]Rehabilitation Medicine Department, University Hospital of Brest, Brest, France

[3]LaTIM, INSERM U1101 Brest, France

[4]Virginia Commonwealth University School of Medicine, Richmond, VA, USA

[5]Mt Washington Pediatric Hospital, Baltimore, MD, USA

Abstract

Background—Obstetrical Brachial Plexus Palsy (OBPP) is a common birth injury, resulting in severe functional losses. Yet, little is known about how OBPP affects the 3D humeral morphology. Thus, the purpose of this study was to measure the 3D humeral architecture in children with unilateral OBPP.

Methods—Thirteen individuals (4F/9M, age=11.8±3.3 years, Mallet score=15.1±3.0) participated in this IRB-approved study. A three-dimensional T1-weighted gradient-recalled-echo magnet resonance image set was acquired for both upper limbs (involved/non-involved). Humeral size, version, and inclination were quantified from 3D humeral models derived from these images.

Results—The involved humeral head was significantly less retroverted and in declination (medial humeral head pointed anteriorly and inferiorly), relative to the non-involved side. Osseous atrophy was present in all three dimensions and affected the entire humerus. The inter-rater reliability was excellent (ICC = 0.96–1.00).

For correspondence and reprints contact: Frances T. Sheehan, PhD, National Institutes of Health, Building 10 CRC RM 1-1469, 10 Center Drive MSC 1604, Bethesda, MD 20892-1604, USA, fsheehan@cc.nih.gov.

All work on for this study was done under protocol number 03-CC-0060, approved by the Institutional Review Board of the National Institute of Child Health and Human Services.

Financial Biases
Frances T. Sheehan, PhD: None
Sylvain Brochard, MD: This work was funded by grants awarded to Dr Brochard from the University Hospital of Brest, the French Society of Physical Medicine and Rehabilitation (SOFMER), the French Society of Research in Children with Disabilities (SFERHE) and by the Intramural Research Program of the National Institutes of Health Clinical Center, Bethesda, MD, USA.
Abrahm Behnam, MS: None
Katharine Alter, MD: None

Discussion—This study demonstrated that both humeral atrophy and bone shape deformities associated with OBPP are not limited to the axial plane, but are three-dimensional phenomena. Incorporating information related to these multiplanar, 3D, humeral deformities into surgical planning could potentially improve functional outcomes following surgery. The documented reduction in retroversion is an osseous adaptation, which may help maintain glenohumeral congruency by partially compensating for the internal rotation of the arm. The humeral head declination is a novel finding and may be an important factor to consider when developing OBPP management strategies, as it has been shown to lead to significant supraspinatus inefficiencies and increased required elevation forces.

Level of evidence—Anatomic Study, Imaging

Keywords

Reliability; Magnetic Resonance Imaging; Shape; Retroversion; Version; Inclination

INTRODUCTION

Obstetrical Brachial Plexus Palsy (OBPP) is a common birth injury, occurring in approximately three in every 1000 births[3; 26; 29; 37]. Children who do not recover completely are left with shoulder muscle imbalance, contracture, disuse, and significant glenoid-humeral deformities[20; 24; 40; 41; 50]. The persisting sequelae are wide ranging, severely restrict the arm function, limit activities of daily living independence [43], and reduce the quality of life for patients and their caregivers[31; 43]. Due to the severity of these persistent sequelae, many children/adolescents with OBPP require extensive rehabilitation and are often referred for invasive interventions and/or surgery[1; 12; 32; 47]. Enhanced knowledge of how the sequelae associated with OBPP affects the three-dimensional (3D) humeral architecture will likely support improved efficacy of OBPP management strategies.

Two-dimensional (2D) glenoid retroversion and glenohumeral subluxation have been well studied in OBPP[10; 21; 23; 27; 34; 37], but few studies have quantified humeral deformity in isolation. The studies that have focused on humeral pathology demonstrated atrophy[28; 37; 38] and “retroversion” on the involved side [46]. These studies were limited to 2D axial- or sagitall-plane analyses. As such, even though humeral deformity is complex and likely three-dimensional; surgical procedures, such as humeral derotation osteotomy[2; 36; 48; 51] and humeral head relocation[36], are being recommended based on limited two-dimensional knowledge. Thus, it is imperative to fill the knowledge gap in regards to how the neurological deficits arising from this birth injury ultimately result in pathological humeral shape. For example, humeral head inclination (equivalent to the femoral neck-shaft angle) has not been measured in children with OBPP. This is a potentially large oversight as changes in humeral head inclination have been shown to limit shoulder function[49] and restoring correct 3D humeral morphology is considered crucial for successful shoulder arthroplasty[17; 18; 25; 39].

Of all the humeral architectural properties, version has been the most well studied, primarily in adults, with a focus on shoulder arthroplasty[6; 17; 22; 25; 39] and overuse-induced injuries[9; 52–55]. Cadaver studies[14; 15; 17; 22; 25; 39] have the advantage of direct investigation

of the 3D bone surfaces, which cannot be performed in living subjects. The 2D measures acquired using X-rays, computed tomography (CT), or magnetic resonance (MR) imaging[6; 8; 13; 16; 19; 46] can be severely affected by the location and orientation of the imaging plane relative to the anatomy studied[7; 16; 17; 42]. Lastly, ultrasound (US)[52–55] is non-ionizing, portable, and less expensive than MR or CT. However, it is a 2D analysis, is highly user-dependent, and relies solely on two closely spaced points of the bicipital groove. Thus, it primarily quantifies bicipital groove axial-plane orientation and not humeral head version. Humeral head inclination has been less well studied[6; 56] and measures in typically developing children and children with OBPP are currently unavailable.

The purpose of this study was to develop a non-invasive methodology for measuring the *in vivo* 3D humeral morphology in individuals with unilateral OBPP in order to test the following hypotheses: 1) The involved humeral head demonstrates significantly decreased retroversion; 2) The articular surface of the involved humeral head is rotated inferiorly; and 3) The involved humerus is atrophic in all three dimensions. For all hypotheses the subject's non-involved arm served as the control. As a test of the clinical utility of the humeral architectural measures, the inter-rater reliability was tested. Lastly, the relationship amongst the morphological parameters, age, functional/impairment levels, and limits to passive external glenohumeral rotation was investigated in order to evaluate the feasibility of predicting functional/impairment levels using a multi-variate regression analysis.

METHODS

Sixteen children/adolescents with unilateral OBPP were recruited for this IRB (intramural IRB of the National Institute of Child Health and Human Development) approved study. Each child/adolescent provided written assent with a legal guardian providing written consent. The single adolescent that was above 18 years of age provided written consent. After consent, a pediatric physiatrist performed a complete history and physical, which included the Mallet[4; 45] and Narakas classification[30] scores, along with the passive ranges of shoulder motion. Three children declined MRI scanning due to fear, complaints of noise, or dizziness and withdrew. The remaining cohort of 13 subjects had an age range of 6.7 to 18.7 years, with four female subjects and five subjects with left side involvement (age = 11.8±3.3 years, height=154.8±21.4 cm, weight=51.8±16.0 kg, Mallet score = 15.1±3.0, Narakas = 2.5±0.8). The average differences (impaired – unimpaired) in shoulder passive range of flexion/extension, abduction, and internal/external rotation were −5.4°±10.3°/−45.4°±16.9°, −11.2°±20.8°, −17.3°±21.5°/−32.7°±−20.3°. For external rotation and extension all subjects demonstrated limited ranges of motion (involved side). For flexion, abduction, and internal rotation six, nine, and four subjects had no side-to-side differences. All other subjects demonstrated reduced ranges of motion (involved side).

Prior to scanning each participant was given time to acclimate to the scanner. The subject was then placed supine on the plinth of a 3T MR scanner (Verio: Siemens, Erlangen, Germany) with the arm as close to anatomic position as possible, but with the forearm pronated and the palm facing the bed for comfort. A standard cardiac coil was placed on the bed (posterior to the shoulder) while its pair was wrapped around the subject's shoulder and chest. When required, in taller subjects, a flexible coil was wrapped around the elbow,

maintaining coverage through the distal humerus. No sedatives or anesthesia were used. To prevent patient or coil movement during scanning, sandbags were placed alongside the arm and a large supportive strap was gently secured around the coils and chest. Both the impaired and unimpaired arms were scanned, but were acquired independently, enabling the shoulder to be positioned at the MR isocenter. A T1-gradient recalled echo sequence was acquired for each shoulder. With the exception of the in-plane field of view, all scanning parameters were held constant across subjects (416 × 312 × 192 pixels, slice thickness 1.2 mm, TR=16.6 msec, TE=5.1 msec, imaging time=4 min 22 sec). This resulted in a slight variation in the in-plane resolution across subjects (0.55–0.63 mm^2), enabling higher resolution for smaller subjects. When needed, a second scan was acquired to capture the distal humerus. The image data were stripped of all identifiers and assigned a random number, blinding the researchers to the subject's identity and to the side of involvement.

A 3D model was created by manually segmenting the outer humeral bone cortex in MIPAV (Medical Image Processing, Analysis and Visualization, NIH, Bethesda, MD, USA). If the growth plate created a discontinuity in the cortical bone surface, the missing surface was approximated by maintaining the curve on either side of the discontinuity. The shapes of the proximal and distal humerus were complex and influenced the study measures more than the shaft. Therefore, every image slice in the humeral head and elbow region was utilized in reconstructing these surfaces. In contrast, the humeral shaft was modeled using every fifth slice. The shaft was defined as the region with minimal image-to-image changes in bone area. A three-dimensional mesh was fitted to the points and then smoothed using an upper deviation limit equal to one half the pixel size in Geomagic (Geomagic Inc, Research Triangle Park, NC, USA). This model was then aligned to its principal axes (Z, Y, and X, Figure 1). X, Y, and Z represented the posterior, left, and superior directions. These axes are calculated based on the distribution of volume within each individual humerus. Thus, the Z-axis (superior) approximately aligned with the medulary axis. This alignment procedure minimized errors associated with visually aligning the humeri[39] and eliminated the dependency between the final measures and the image plane location/orientation[7; 16; 17; 42]. The anatomic planes were defined based on this alignment (Figure 1).

As part of defining the 3D humeral architecture, a series of points were defined. First, Pcut (a point on the metaphyseal junction) was determined as the inflection point of the head curvature as it joins with the shaft (Figure 2). Next, the greater and lesser tuberosity points (GT and LT, Figure 1) were defined as the points along the greater and lesser tuberosity that were most distant from the humeral head center in the anterior-posterior and medial-lateral directions. The center of the bicipital groove (BG, Figure 1) was defined as the deepest point of the bicipital groove at the average superior-inferior location of GT and LT. The model was then converted back into a point cloud (20,000 pts).

An in-house Matlab code was used to compute the 3D humeral architectural parameters based on the model's point cloud, LT, GT, BG, and Pcut. First, the magnitude and direction of the three radii (R1, R2, and R3, Figure 3) of the best-fit ellipsoid to all points superior of Pcut (metaphyseal junction) was quantified. R1, R2, and R3 represented the radii of the ellipsoid in descending order of size. The humeral head center (HC) was defined by the center of this ellipsoid. As a measure of humeral head distortion, the ratios of the radii were

calculated (R1/R2, R1/R3, and R2/R3). Next, the most superior and inferior humeral points (PS and PI, Figure 4) and the most lateral and medial points on the elbow's epicondylar axis (Lepi and Mepi, Figure 2) were defined. Humeral length (Figure 4) was defined as the distance between the PS and PI. The axis of the humeral shaft (ShaftAxis) was defined as the center of a best-fit cylinder fitted to the "cylindrical" portion of the shaft. This portion was defined as between a plane 33% of the humeral length superior to PI and a plane 17% of the humeral length distal to PS, based on the work of Descamps and colleagues[11]. The epicondylar axis (EpiAxis) was defined as the axis from Lepi to Mepi and its length was the epicondylar width. Retroversion (Figure 3) was measured relative to the EpiAxis, but four reference axes were used: 1) the vector **R1**; 2) the vector from BC to HC 3) the vector from LT to HC; and 4) the vector from LT to a point on the shaft axis at the same superior-inferior level as LT. These four angles (verR1, verBC_HC, verLT_HC, and verLT_shaft, respectively) were measured as a projection into the axial plane. Mathematically, a positive version angle (Figure 3) indicated humeral head internal rotation and was termed retroversion, following typical conventions. The inclination of the head was defined as the angle (projected into the coronal plane) of R1 relative to both the ShaftAxis and the EpiAxis (head_incl_shaft and head_incl_epi, Figure 4). A side-to-side difference in head_incl_epi and head_incl_shaft angle greater than 0°, indicated inclination (medial humeral head pointed superiorly). The opposite was considered declination. Multiple angles were used to define version and inclination in order to support comparisons with past and future studies.

All measures, beginning with bone segmentation, were completed by a single examiner (S.B.). Then, 11 datasets were selected at random for an inter-rater reliability test (5 were from the non-involved side and 6 were from the involved side). A second researcher (A.J.B.), blinded to the results of the primary analysis, segmented these 11 datasets and repeated the morphological analysis. A second set of images was not acquired to minimize the subject's time within the MR unit and because it was deemed unnecessary. The analysis was based on the quantification of the complete bone surface, making the final measures insensitive to image plane orientation and location. This would not be the case if the measures were acquired in a single 2D slice[7; 16; 17; 42].

An a priori power analysis determined that 13 subjects were required (α= 0.05 and β=0.8) to determine a similar difference in version between the impaired and unimpaired side as published previously[46]. The variables of interest were compared using a paired one-tailed Student's t-test. Understanding that the numerous tests could produce a type 1 error, a Bonferroni false discovery rate (FDR) correction[5] was used. Intra-class correlation coefficients (ICCs), using a two-way mixed effects model, were computed to evaluate inter-rater reliability of the 3D humeral shape parameters. The 3D morphological parameters were correlated with each other and age for the non-involved limb. A similar analysis was run for the side-to-side differences in morphological parameters. Lastly, a multi-regression analysis was run to determine if functional and impairment level (Mallet and Narakas) along with the change in the passive range of external rotation could be predicted by the side-to-side differences in humeral morphological parameters. A p-value < 0.05 was considered significant. The multi-regression analysis was isolated to the difference in the passive range of external rotation, as internal contractures are most common in OBPP.

Results

The involved arm was less retroverted (more externally rotated) than the non-involved arm (−17.2° to −23.6°, Table 1). Two subjects demonstrated the opposite (increased retroversion on the involved side). The variability across subjects was greater on the involved side. Retroversion was not correlated with age (non-involved arm, r=0.52–0.56, p=0.052–0.085, Table 2). The correlation amongst the version angles and amongst the side-to-side differences in version (Table 3) ranged from moderate to strong.

The involved humeral head was in declination (−4.4° to −6.1°, Table 1), in comparison to the non-involved arm. These results are presented with a single subject removed, as the subject was deemed to be an outlier. For this subject the difference in inclination (an increase of 24.4° and 26.6° on the involved side) was greater than 2.5 standard deviations away from the average side-to-side difference. This subject's neurologic injury and functional impairments were the most severe of all the subjects. Inclusive of this subject, only three subjects demonstrated inclination on the involved side. The two inclination angles were moderately to strongly correlated with each other on the non-involved side (r=0.65, p=0.023, Table 2). Yet, no correlation existed between the side-to-side differences of these two angles (Table 3). Head_inl_epi decreased with age (non-involved side, r = −0.71, p=0.009, Table 2).

All size parameters (Table 4) were smaller on the involved side. The largest percent change between sides was in R3 (−15.4%) and epicondylar width (−13.5%). The ratios of R1/R3 and R2/R3 were smaller on the involved side, indicating that the humeral head proximal-to-distal size was foreshortened relative to the already reduced dimensions in the medial-lateral and anterior-posterior directions. Thus, the involved side was more elliptical in shape when compared to the non-involved side. Atrophy of the involved side was consistent across all subjects, with one exception; R2 was 0.4 mm larger on the involved side for one subject. The size parameters were strongly correlated with each other (non-involved side, r = 0.83–0.99, p≤0.001). The size parameters were all moderately to strongly correlated with age (non-involved side, 0.71–0.86, p≤0.007).

The Mallet score was moderately correlated with the side-to-side difference in epicondylar width and head_incl_epi, whereas the Narakas score and the difference in passive external rotation were not correlated with any morphological parameter (Table 4). Using a multi-regression analysis did not greatly improve the predictability of the Mallet score over using epicondylar width and head_incl_epi individually (r^2 = 0.57–0.58, p<0.003). Yet, together the side-to-side differences in verR1 and head_incl_shaft were able to explain 56% of the variability in Narakas score:

$$\mathrm{Narakas} = 34.25 + 0.165 * \mathrm{verR1} + 0.462 * \mathrm{head\_incl\_shaft}\ (r^2 = 0.56, p = 0.025)$$

The reliability for all measures was excellent, ranging from 0.960–1.000 (p<0.001, Table 5). This was well above the value of 0.90 that is needed for "reasonable clinical validity"[35]. A post-hoc power analysis revealed that sufficient power was achieved for all side-to-side

comparisons of the humeral morphological parameters (β>0.80). If a 2-tailed analysis was used, the conclusions did not change, but the power slipped slightly (0.52<β>0.80).

DISCUSSION

This study is the first to evaluate and report 3D humeral shape changes in children with OBPP. In doing so, it demonstrates this birth injury leads to morphological changes affecting the entire humerus, as well as osseous atrophy in all three dimensions. These changes result in the humeral head being rotated externally and declined inferiorly. The documented 3D humeral shape deformations are likely related to the well reported glenohumeral subluxation, glenoid version, and the internally rotated arm posture at rest. Given the variability in the results across subjects,. incorporating information related to these 3D humeral deformities into surgical planning may foster improved functional outcomes.

It is difficult to compare version across studies due to variable anatomical references, as well as to the fact that the precise definition is often not reported. One study measured version as the angle between a vector defining the anterior surface of the elbow relative to a fixed horizontal line[39], whereas another used both axial and sagittal plane references to measure version[54]. In general, most studies have used an angle (projected into the axial plane) between the epicondylar axis and a vector associated with the humeral head. Another point of confusion is that the direction of rotation represented by the term “retroversion” or “retrotorsion” has not been clearly defined or agreed upon. Most studies define an internal rotation of the humeral head as retroversion/retrotorsion, yet some studies have defined this rotation as anteversion[46]. Two of the version angles used in the current study (verBG_HC and verHC_HC) referenced the humeral head center. The HC was used, instead of more commonly used center of the articulation, since the 3D cartilage boundary is often difficult to identify[6]. This is particularly true in MR images of young children with unfused humeri and in the presence of osseous deformities. Although not previously used in the literature, verR1 has the advantage of being calculated based on the entire set of humeral head points (4,000–5,000) and not just two points (e.g., LT, BG, and GT), which can be altered in pathology and are more sensitive to identification errors.

The severe impact on humeral morphology induced by the sequelae of OBPP can be seen in the side-to-side differences in retroversion (average change in version ranged from −17.2° to −23.6°), which is approximately twice that seen when comparing the throwing and non-throwing arm of overhand sports athletes (average difference between sides ranged from 10.6° to 11.2°)[9; 53; 54]. The decreased humeral head retroversion in the current cohort coupled with the decreased passive and active external shoulder rotation typically reported for OBPP[41; 44] mirrors the increased retroversion with decreased active internal rotation in athletes of overhand sports[52]. The large differences in version seen in the current study must be balanced against much smaller differences (Δ=10.3°) reported previously for a similar population[46]. The variation between these studies is likely due to methodological differences (2D vs 3D) and to the severity of impairment in the current, as compared to the past, study (average Narakas classification = 2.5 versus 1.5).

Humeral retroversion on the involved side was 11.2° less than that reported previously in 185 skeletally matured dried bones (verLT_Shaft=65.3° versus 74.4° [22]). In contrast, retroversion in the non-involved arm was 12.1° greater than that measured previously (verLT_Shaft=88.8° versus 74.4° [22]). VerLT_Shaft was equal to the sum of EP and LT in the previous dried bone study[22]. The increased retroversion on the non-involved side (as compared to adult values) supports the previously published model that the humerus begins retroverted at birth and this retroversion diminishes throughout childhood[14; 15]. Thus, the lack of a significant correlation between retroversion and age was likely due to insufficient power. The decreased retroversion on the involved side (compared to the adult values) suggests that following the birth injury the humerus rapidly loses the in utero retroversion[15] to quickly arrive at an anteverted position. This is in contrast to the typically developing child who progresses to a less retroverted morphology more slowly, throughout childhood, reaching adult values at approximately 16 years of age. This decreased retroversion also suggests an osseous compensation to maintain glenoid-humeral congruency in a limb that is in an internally rotated position due to muscle strength imbalance. Unfortunately, this decreased retroversion leads to an increase in the internally rotated arm posture by further decreasing the available degrees for external rotation.

Humeral head declination in OBPP is a finding novel to this study and may be a key morphological parameter when considering the functional losses associated with OBPP. Voight and colleagues demonstrated that when such a deformity was created in cadavers, the supraspinatus efficiency was decreased and the forces required for arm elevation increased[49]. Thus, neurological deficits resulting from the birth injury lead to muscle atrophy/contractures, which promotes boney deformations; and these boney deformations appear to circle back and further weaken the shoulder complex. The unexplained variance between the two inclination angles on the non-involved side and the lack of correlation in the side-to-side changes of these two angles suggests that the declination originates from rotation of both the head and elbow relative to the shaft. As the difference in inclination between sides was significant only after a single outlier was removed, there may be subgroups in the OBPP population that demonstrate osseous deformities opposite to the “average” individual with OBPP. This reinforces the fact that individual patient variability should be considered when recommending procedures and may account in part for differences in successful functional outcomes following surgery.

Humeral head inclination was based on the 3D orientation of the entire humeral head surface to avoid problems with indistinct cartilage boundaries[6], particularly in skeletally immature humeri and those affected by pathology. In contrast, past in vivo studies have focused solely on adults, have used both 2D[33] and 3D[56] analyses, and have determined the humeral head orientation based on the cartilage surface. As this study demonstrated a declination of the humeral head with development, comparisons to such previous data may not lend many insights. Future studies supporting or refuting the correlation between age and humeral head inclination would likely provide further insights into shoulder development, morphology, pathology, and injuries.

The documented humeral atrophy lends insights into the sequelae of OBPP and matched well with previous data[28]. The ratio of humeral length (involved/non-involved = 93.7%) was

nearly identical to that reported previously (93%[28]). This osseous atrophy is not limited to the head, but extended through the shaft to the elbow. For example, the epicondylar width demonstrates the second highest percent change in length. Similarly, the significantly decreased radii of the best fit humeral head ellipsoid and the increased ratios of R1/R3 and R2/R3 on the involved side demonstrate that the entire humeral head experiences atrophy, but this atrophy is greatest in the superior-inferior direction, making the humeral head of the involved side more elliptical than the non-involved. This shape variation may influence the likelihood of dislocation.

The decision to use the non-involved side as a control could be seen as controversial. While two studies have demonstrated differences[6; 55] in version between sides, the majority of studies found no differences[15; 22; 39; 52], including one based on 180 dried humeri of children[15]. Further, the studies reporting differences in version indicated that the right side was more retroverted (8.9°–10.5°). This is approximately half the difference found in the current study. Thus, using the non-involved arm as a control was deemed to be both appropriate and desirable, as it provided an exact age, sex, height, and weight match.

The fact that over 50% of the Mallet score could be predicted by either humeral atrophy or the side-to-side difference in inclination clearly indicates that humeral morphological changes impact function in OBPP. The remaining unexplained variability is most likely attributable to glenoid architectural changes, muscle atrophy, and muscle contractures. The relationship between the Narakas score and the side-to-side differences in both version and inclination indicates that these differences are greater when the initial injury is more severe, which is as expected. The fact that the inclination angle was associated with both the Mallet and the Narakas scores again highlights the importance of this angle in OBPP. The lack of correlation between the study measures and the difference in passive range of external rotation likely resulted from the fact that multiple factors in OBPP can limit passive external rotation and that these relationships may be non-linear. The correlations also provided a validation of the methods. All four measures of version define the same property. Thus, a strong correlation between them should be expected and this is what was found. The exception being the moderate correlations between verR1 and the other version angles, which indicates that this angle is somewhat independent to the other three. It would be expected that all size measurements correlate with age, and strong correlations were found here as well. There is evidence in the literature that humeral retroversion is inversely correlated with age. The correlation analysis of the non-involved arm suggests, but does not prove, that both retroversion and the side-to-side differences in retroversion are inversely correlated with age, but further investigation is needed. Novel to the study, the correlations revealed that the humeral head declined through development.

Although developed as a research tool, the current 3D methodology can be easily adapted to clinical use, potentially providing improved reliability, a reduction in the time required to obtain measures, and a more complete description of subject-specific morphological changes. Most pre-surgical planning includes acquiring a 3D CT or MR image set of both shoulders. If the elbow was added to the scan, then the same modeling and measurement procedure could be applied. With a CT image set, the segmentation process could be automated, eliminating the most temporally costly step of the current analysis. Once the 3D

humeral model had been generated, a complete description of the 3D shape deformities and atrophy could be quantified automatically using readily available computational codes. For example, verR1 has excellent reliability and correlated well with the three other version angles. It did not require the subjective evaluation of numerous individual points; eliminating the sensitivity of the final measures to image plane orientation and location[7; 16; 17]. The latter implies that variations in patient position relative to the magnet would not propagate into the final measures. Even though there is a clear path to acquiring 3D morphology using standard clinical imaging, the relationship between 2D and 3D humeral shape parameters should be examined to help support cross-study and cross-center comparisons. As two subjects demonstrated a retroverted head and three subjects demonstrated an increase in inclination on the involved side, a full understanding of the subject-specific 3D, multi-planar, humeral deformities may help maximize functional improvements when these individuals undergo invasive procedures.

This study was delimited to the use of MR imaging, which primarily limited the cohort size and power. The use of CT would have automated the 3D model generation, and thereby allow for a larger study cohort, but exposing these young subjects to ionizing radiation, could not be justified for a pure research study. The use of MR also limited the lower age range, as sedation could not be justified for a research study.

CONCLUSIONS

Improvements in the treatment of children with OBPP will be fostered by a more advanced and accurate understanding of the osseous deformations associated with the long term neurologic sequelae arising from the initial injury. It is crucial to not only document these osseous deformations, but to evaluate how these architectural changes may create a feedback loop, causing greater functional losses. To that end, this study demonstrated that the humeral head was externally rotated and in declination on the involved side of children/adolescents with unilateral OBPP. In addition, atrophy in all three-dimensions at both the head and elbow were documented. The currently reported morphological changes also likely cause alterations to the moment arms of the shoulder muscles attaching into the humerus. An analysis of moment arms was beyond the scope of the current study, but warrants further investigation. The currently applied methodology is easily adaptable to clinical use, as 3D images are typically part of pre-surgical planning. Thus, adding a 3D analysis of humeral morphology to surgical planning in OBPP may help maximize functional gains. In addition, future studies relating 2D measures to 3D humeral morphology are needed to support cross-center and cross-study comparisons.

Acknowledgments

The authors would like to thank Diane Damiano, PhD, Christopher Hollingsworth, Lindsay Curatalo, Christopher Stanley, and Lori Ohlrich for her help and support in the work. In addition, we would like to thank the Radiology Department, headed by Dr. David Bluemke at the Clinical Center of the National Institutes of Health for their support of this work. This work was by the Intramural Research Program of the National Institutes of Health Clinical Center, Bethesda, MD, USA and Dr. Brochard was supported by an award from the University Hospital of Brest, the French Society of Physical Medicine and Rehabilitation (SOFMER), the French Society of Research in Children with Disabilities (SFERHE).

References

1. Abzug JM, Chafetz RS, Gaughan JP, Ashworth S, Kozin SH. Shoulder function after medial approach and derotational humeral osteotomy in patients with brachial plexus birth palsy. J Pediatr Orthop. 2010; 30:469–74. http://dx.doi.org/10.1097/BPO.0b013e3181df8604. [PubMed: 20574265]
2. al Zahrani S. Modified rotational osteotomy of the humerus for Erb's palsy. International orthopaedics. 1993; 17:202–4. [PubMed: 8340179]
3. Backe B, Magnussen EB, Johansen OJ, Sellaeg G, Russwurm H. Obstetric brachial plexus palsy: a birth injury not explained by the known risk factors. Acta obstetricia et gynecologica Scandinavica. 2008; 87:1027–32. http://dx.doi.org/10.1080/00016340802415648. [PubMed: 18798052]
4. Bae DS, Waters PM, Zurakowski D. Reliability of three classification systems measuring active motion in brachial plexus birth palsy. J Bone Joint Surg Am. 2003; 85-A:1733–8. http://dx.doi.org/10.2519/jospt.2007.2449. [PubMed: 12954832]
5. Benjamini Y, Hochberg Y. Controlling the False Discovery Rate - a Practical and Powerful Approach to Multiple Testing. J Roy Stat Soc B Met. 1995; 57:289–300.
6. Boileau P, Bicknell RT, Mazzoleni N, Walch G, Urien JP. CT scan method accurately assesses humeral head retroversion. Clin Orthop Relat Res. 2008; 466:661–9. http://dx.doi.org/10.1007/s11999-007-0089-z. [PubMed: 18264854]
7. Bokor DJ, O'Sullivan MD, Hazan GJ. Variability of measurement of glenoid version on computed tomography scan. J Shoulder Elbow Surg. 1999; 8:595–8. [PubMed: 10633895]
8. Cassagnaud X, Maynou C, Petroff E, Dujardin C, Mestdagh H. A study of reproducibility of an original method of CT measurement of the lateralization of the intertubercular groove and humeral retroversion. Surg Radiol Anat. 2003; 25:145–51. http://dx.doi.org/10.1007/s00276-003-0101-6. [PubMed: 12690519]
9. Chant CB, Litchfield R, Griffin S, Thain LM. Humeral head retroversion in competitive baseball players and its relationship to glenohumeral rotation range of motion. J Orthop Sports Phys Ther. 2007; 37:514–20. http://dx.doi.org/10.2519/jospt.2007.2449. [PubMed: 17939610]
10. Clarke SE, Kozin SH, Chafetz RS. The biceps tendon as a measure of rotational deformity in residual brachial plexus birth palsy. J Pediatr Orthop. 2009; 29:490–5. http://dx.doi.org/10.1097/BPO.0b013e3181aa9407. [PubMed: 19568023]
11. Descamps S, Moreel P, Garcier JM, Bouillet B, Brehant J, Tanguy A. Existence of a rotational axial component in the human humeral medullary canal. Surg Radiol Anat. 2009; 31:579–83. http://dx.doi.org/10.1007/s00276-009-0485-z. [PubMed: 19277447]
12. Desiato MT, Risina B. The role of botulinum toxin in the neuro-rehabilitation of young patients with brachial plexus birth palsy. Pediatric rehabilitation. 2001; 4:29–36. [PubMed: 11330848]
13. Doyle AJ, Burks RT. Comparison of humeral head retroversion with the humeral axis/biceps groove relationship: a study in live subjects and cadavers. J Shoulder Elbow Surg. 1998; 7:453–7. [PubMed: 9814921]
14. Edelson G. Variations in the retroversion of the humeral head. J Shoulder Elbow Surg. 1999; 8:142–5. [PubMed: 10226966]
15. Edelson G. The development of humeral head retroversion. J Shoulder Elbow Surg. 2000; 9:316–8. http://dx.doi.org/10.1067/mse.2000.106085. [PubMed: 10979528]
16. Farrokh D, Fabeck L, Descamps PY, Hardy D, Delince P. Computed tomography measurement of humeral head retroversion: influence of patient positioning. J Shoulder Elbow Surg. 2001; 10:550–3. http://dx.doi.org/10.1067/mse.2001.118412. [PubMed: 11743534]
17. Harrold F, Wigderowitz C. A three-dimensional analysis of humeral head retroversion. J Shoulder Elbow Surg. 2012; 21:612–7. http://dx.doi.org/10.1016/j.jse.2011.04.005. [PubMed: 21783384]
18. Hasan SS, Leith JM, Campbell B, Kapil R, Smith KL, Matsen FA 3rd. Characteristics of unsatisfactory shoulder arthroplasties. J Shoulder Elbow Surg. 2002; 11:431–41. http://dx.doi.org/10.1067/mse.2002.125806. [PubMed: 12378161]
19. Hill JA, Tkach L, Hendrix RW. A study of glenohumeral orientation in patients with anterior recurrent shoulder dislocations using computerized axial tomography. Orthopaedic review. 1989; 18:84–91. [PubMed: 2915913]

20. Hoeksma AF, Ter Steeg AM, Dijkstra P, Nelissen RG, Beelen A, de Jong BA. Shoulder contracture and osseous deformity in obstetrical brachial plexus injuries. J Bone Joint Surg Am. 2003; 85-A:316–22. [PubMed: 12571311]
21. Hogendoorn S, van Overvest KL, Watt I, Duijsens AH, Nelissen RG. Structural changes in muscle and glenohumeral joint deformity in neonatal brachial plexus palsy. J Bone Joint Surg Am. 2010; 92:935–42. http://dx.doi.org/10.2106/JBJS.I.00193. [PubMed: 20360518]
22. Hromadka R, Kubena AA, Pokorny D, Popelka S, Jahoda D, Sosna A. Lesser tuberosity is more reliable than bicipital groove when determining orientation of humeral head in primary shoulder arthroplasty. Surg Radiol Anat. 2010; 32:31–7. http://dx.doi.org/10.1007/s00276-009-0543-6. [PubMed: 19693428]
23. Kozin SH. Correlation between external rotation of the glenohumeral joint and deformity after brachial plexus birth palsy. J Pediatr Orthop. 2004; 24:189–93. http://dx.doi.org/10.1097/01241398-200403000-00011. [PubMed: 15076606]
24. Kozin SH. The evaluation and treatment of children with brachial plexus birth palsy. J Hand Surg Am. 2011; 36:1360–9. http://dx.doi.org/10.1016/j.jhsa.2011.05.018. [PubMed: 21816296]
25. Kummer FJ, Perkins R, Zuckerman JD. The use of the bicipital groove for alignment of the humeral stem in shoulder arthroplasty. J Shoulder Elbow Surg. 1998; 7:144–6. [PubMed: 9593093]
26. Lagerkvist AL, Johansson U, Johansson A, Bager B, Uvebrant P. Obstetric brachial plexus palsy: a prospective, population-based study of incidence, recovery, and residual impairment at 18 months of age. Dev Med Child Neurol. 2010; 52:529–34. http://dx.doi.org/10.1111/j.1469-8749.2009.03479.x. [PubMed: 20041937]
27. Lippert WC, Mehlman CT, Cornwall R, Foad MB, Laor T, Anton CG, et al. The intrarater and interrater reliability of glenoid version and glenohumeral subluxation measurements in neonatal brachial plexus palsy. J Pediatr Orthop. 2012; 32:378–84. http://dx.doi.org/10.1097/BPO.0b013e31825611bd. [PubMed: 22584839]
28. McDaid PJ, Kozin SH, Thoder JJ, Porter ST. Upper extremity limb-length discrepancy in brachial plexus palsy. J Pediatr Orthop. 2002; 22:364–6. http://dx.doi.org/10.1097/01241398-200205000-00019. [PubMed: 11961456]
29. Mollberg M, Lagerkvist AL, Johansson U, Bager B, Johansson A, Hagberg H. Comparison in obstetric management on infants with transient and persistent obstetric brachial plexus palsy. Journal of child neurology. 2008; 23:1424–32. http://dx.doi.org/10.1177/0883073808320620. [PubMed: 19073848]
30. Narakas, AO. Obstetrical brachial plexus injuries. In: Lamb, D., editor. The Paralysed Hand. Edinburgh: Churchill Livingstone; 1987. p. 116-35.
31. Oskay D, Oksuz C, Akel S, Firat T, Leblebicioglu G. Quality of life in mothers of children with obstetrical brachial plexus palsy. Pediatrics international: official journal of the Japan Pediatric Society. 2012; 54:117–22. http://dx.doi.org/10.1111/j.1442-200X.2011.03455.x. [PubMed: 21883689]
32. Ozturk K, Bulbul M, Demir BB, Buyukkurt CD, Ayanoglu S, Esenyel CZ. Reconstruction of shoulder abduction and external rotation with latissimus dorsi and teres major transfer in obstetric brachial plexus palsy. Acta orthopaedica et traumatologica turcica. 2010; 44:186–93. http://dx.doi.org/10.3944/AOTT.2010.2332. [PubMed: 21088458]
33. Pape G, Bruckner T, Loew M, Zeifang F. Treatment of severe cuff tear arthropathy with the humeral head resurfacing arthroplasty: two-year minimum follow-up. J Shoulder Elbow Surg. 2013; 22:e1–7. http://dx.doi.org/10.1016/j.jse.2012.04.006. [PubMed: 22743073]
34. Pedowitz DI, Gibson B, Williams GR, Kozin SH. Arthroscopic treatment of posterior glenohumeral joint subluxation resulting from brachial plexus birth palsy. J Shoulder Elbow Surg. 2007; 16:6–13. http://dx.doi.org/10.1016/j.jse.2006.04.008. [PubMed: 17055299]
35. Portney, L.; Watkins, M. Foundations of Clinical Research Applications to Practice. 2009. Statistical Measures of Reliability; p. 514
36. Poyhia T, Lamminen A, Peltonen J, Willamo P, Nietosvaara Y. Treatment of shoulder sequelae in brachial plexus birth injury. Acta orthopaedica. 2011; 82:482–8. http://dx.doi.org/10.3109/17453674.2011.588855. [PubMed: 21657969]

37. Poyhia TH, Lamminen AE, Peltonen JI, Kirjavainen MO, Willamo PJ, Nietosvaara Y. Brachial plexus birth injury: US screening for glenohumeral joint instability. Radiology. 2010; 254:253–60. http://dx.doi.org/10.1148/radiol.09090570. [PubMed: 20032156]
38. Reading BD, Laor T, Salisbury SR, Lippert WC, Cornwall R. Quantification of humeral head deformity following neonatal brachial plexus palsy. J Bone Joint Surg Am. 2012; 94(1–8):e136. http://dx.doi.org/10.2106/JBJS.K.00540. [PubMed: 22992884]
39. Robertson DD, Yuan J, Bigliani LU, Flatow EL, Yamaguchi K. Three-dimensional analysis of the proximal part of the humerus: relevance to arthroplasty. J Bone Joint Surg Am. 2000; 82-A:1594–602. [PubMed: 11097450]
40. Ruchelsman DE, Grossman JA, Price AE. Glenohumeral deformity in children with brachial plexus birth injuries. Bull NYU Hosp Jt Dis. 2011; 69:36–43. [PubMed: 21332437]
41. Shenaq SM, Bullocks JM, Dhillon G, Lee RT, Laurent JP. Management of infant brachial plexus injuries. Clinics in plastic surgery. 2005; 32:79–98. ix. http://dx.doi.org/10.1016/j.cps.2004.09.001. [PubMed: 15636767]
42. Shibanuma N, Sheehan FT, Lipsky PE, Stanhope SJ. Sensitivity of femoral orientation estimates to condylar surface and MR image plane location. J Magn Reson Imaging. 2004; 20:300–5. http://dx.doi.org/10.1002/jmri.20106. [PubMed: 15269957]
43. Strombeck C, Fernell E. Aspects of activities and participation in daily life related to body structure and function in adolescents with obstetrical brachial plexus palsy: a descriptive follow-up study. Acta Paediatr. 2003; 92:740–6. http://dx.doi.org/10.1111/j.1651-2227.2003.tb00611.x. [PubMed: 12856989]
44. Uhing MR. Management of birth injuries. Clinics in perinatology. 2005; 32:19–38. v. http://dx.doi.org/10.1016/j.clp.2004.11.007. [PubMed: 15777819]
45. van der Sluijs JA, van Doorn-Loogman MH, Ritt MJ, Wuisman PI. Interobserver reliability of the Mallet score. Journal of pediatric orthopedics Part B. 2006; 15:324–7. http://dx.doi.org/10.1097/01202412-200609000-00004. [PubMed: 16891958]
46. van der Sluijs JA, van Ouwerkerk WJ, de Gast A, Wuisman P, Nollet F, Manoliu RA. Retroversion of the humeral head in children with an obstetric brachial plexus lesion. J Bone Joint Surg Br. 2002; 84:583–7. http://dx.doi.org/10.1302/0301-620X.84B4.12243. [PubMed: 12043783]
47. Vekris MD, Lykissas MG, Beris AE, Manoudis G, Vekris AD, Soucacos PN. Management of obstetrical brachial plexus palsy with early plexus microreconstruction and late muscle transfers. Microsurgery. 2008; 28:252–61. http://dx.doi.org/10.1002/micr.20493. [PubMed: 18381657]
48. Vilaca PR Jr, Uezumi MK, Zoppi Filho A. Centering osteotomy for treatment of posterior shoulder dislocation in obstetrical palsy. Orthopaedics & traumatology, surgery & research: OTSR. 2012; 98:199–205. http://dx.doi.org/10.1016/j.otsr.2011.09.019.
49. Voigt C, Kreienborg S, Megatli O, Schulz AP, Lill H, Hurschler C. How does a varus deformity of the humeral head affect elevation forces and shoulder function? A biomechanical study with human shoulder specimens. Journal of orthopaedic trauma. 2011; 25:399–405. http://dx.doi.org/10.1097/BOT.0b013e31820beb80. [PubMed: 21637119]
50. Waters PM. Update on management of pediatric brachial plexus palsy. Journal of pediatric orthopedics Part B. 2005; 14:233–44. http://dx.doi.org/10.1097/01202412-200507000-00001. [PubMed: 15931025]
51. Waters PM, Bae DS. The effect of derotational humeral osteotomy on global shoulder function in brachial plexus birth palsy. J Bone Joint Surg Am. 2006; 88:1035–42. http://dx.doi.org/10.2106/jbjs.e.00680. [PubMed: 16651578]
52. Whiteley R, Ginn K, Nicholson L, Adams R. Indirect ultrasound measurement of humeral torsion in adolescent baseball players and non-athletic adults: reliability and significance. Journal of science and medicine in sport/Sports Medicine Australia. 2006; 9:310–8. http://dx.doi.org/10.1016/j.jsams.2006.05.012. [PubMed: 16807103]
53. Wyland DJ, Pill SG, Shanley E, Clark JC, Hawkins RJ, Noonan TJ, et al. Bony adaptation of the proximal humerus and glenoid correlate within the throwing shoulder of professional baseball pitchers. The American journal of sports medicine. 2012; 40:1858–62. http://dx.doi.org/10.1177/0363546512452720. [PubMed: 22785605]

54. Yamamoto N, Itoi E, Minagawa H, Urayama M, Saito H, Seki N, et al. Why is the humeral retroversion of throwing athletes greater in dominant shoulders than in nondominant shoulders? J Shoulder Elbow Surg. 2006; 15:571–5. http://dx.doi.org/10.1016/j.jse.2005.06.009. [PubMed: 16979051]

55. Yoshida M, Saho Y, Katayose M. Reliability of measuring humeral retroversion using ultrasound imaging in a healthy nonthrowing population. Journal of sport rehabilitation. 2010; 19:149–60. [PubMed: 20543216]

56. Zhang L, Yuan B, Wang C, Liu Z. Comparison of anatomical shoulder prostheses and the proximal humeri of Chinese people. Proceedings of the Institution of Mechanical Engineers Part H, Journal of engineering in medicine. 2007; 221:921–7.

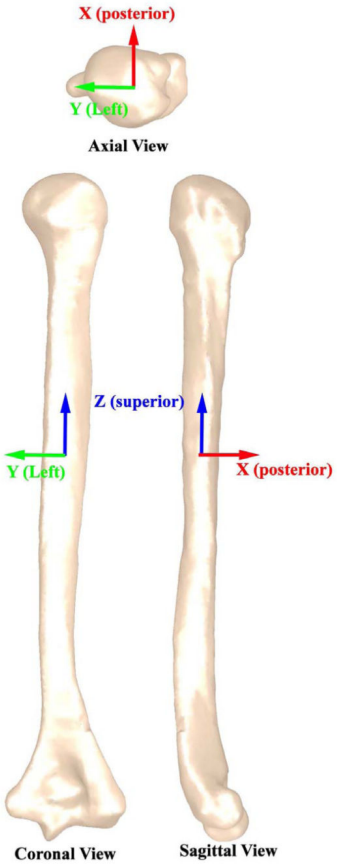

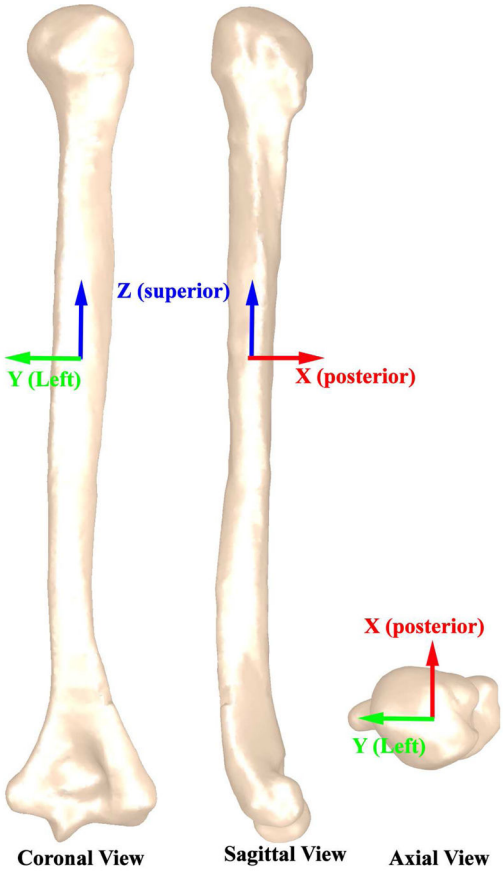

Figure 1. Principal axes and Cardinal planes

The principal axes are defined as three mutually perpendicular axes about which the moment of inertia of the humerus is maximized (http://oxforddictionaries.com/definition/english/principal-axis) and define the distribution of shape within the humerus. Of the three axes, the first principal axis (**Z** – superior direction) has the largest moment or inertia and the third principal axis (**X** – posterior direction) has the smallest moment of inertia. The cardinal planes were defined based on the principal axes, the coronal plane was perpendicular to **X**, the sagittal plane was perpendicular to **Y**, and the axial plane was perpendicular to **Z**.

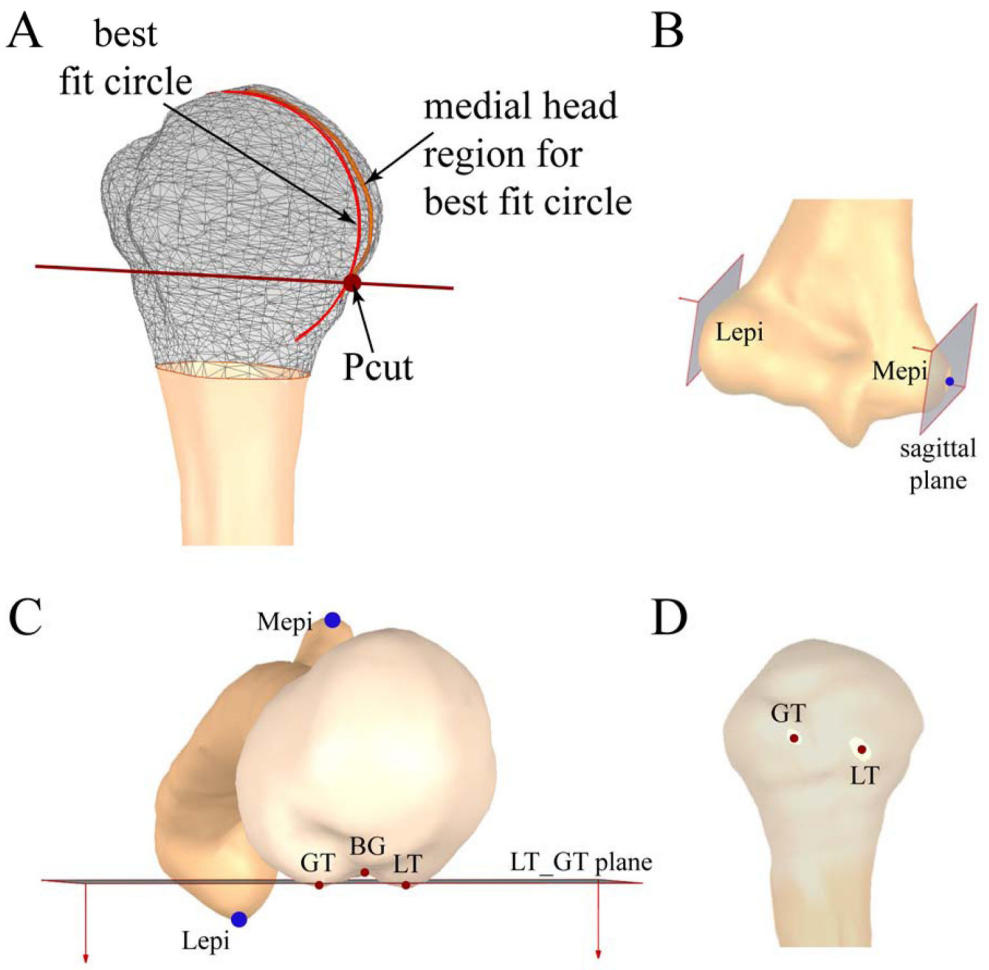

Figure 2. Defining points of interest

A: The humeral head cut-off point (Pcut, metaphyseal junction) was identified by an isolated 2 mm thick section of the center (anterior-posterior) of the medial humerus. The fitting section ("medial head region for the best fit circle") was defined as the section medial to the most superior humeral point and just inferior to the visually determined inflection point between the head and shaft. Pcut was defined as the location where the best-fit circle to the fitting section intersected the fitting section on the inferior medial side. **B:** The medial and lateral epicondyle points (Mepi and Lepi) were defined as the most medial and lateral points of the elbow epicondylar axis. **C& D** The greater and lesser tuberosity points (GT and LT) were defined by establishing an XZ-plane (sagittal plane) and then translating and rotating (about the superior-inferior axis) the plane until the plane "cut-off" the sections of the greater and lesser tuberosity that were furthest from the humeral head center. The center of each of these sections was defined as GT and LT. BG (bicipital groove point) was defined as the deepest point in the groove at the average superior-inferior location of GT and LT.

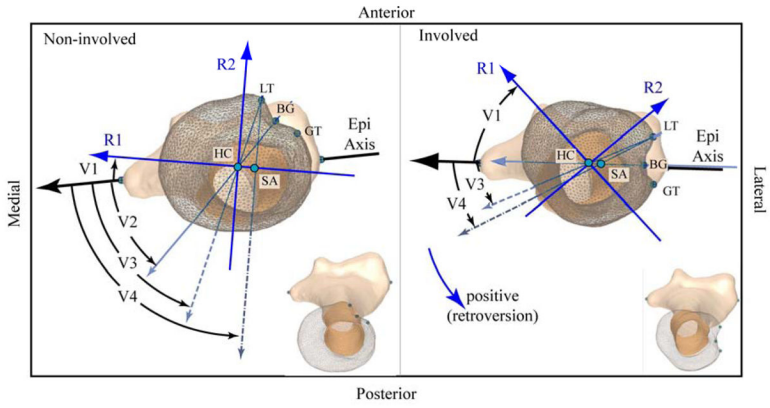

Figure 3. Version

The non-involved left (left box) and involved right (right box) humerii from a single subject (subject 8, the same as in Figure 4), as viewed in a pure axial view (after humerii were aligned with the principal axes). A mirror image was created of the non-involved left arm (making it appear as a right arm) for direct visual comparison. Both images are scaled identically. An oblique view of each humerii is provided in the bottom right in order to provide perspective. Retroversion is positive for internal rotation of the humeral head relative to the epicondylar axis (Epi Axis); the medial humeral head rotates posteriorly. **R1**, **R2**, and **R3** are the primary, secondary and tertiary radii of the best fit ellipsoid to the humeral head, but are shown with extended lengths for visualization purposes. **R3** is mutual perpendicular to **R1** and **R2** and is not shown for clarity. Version is measured relative to the Epi Axis. The reference axis for each angle is as follows: **V1** (verR1): the first (maximum) radii of the best fit ellipsoid to the humeral head (R1); **V2** (verBG_HC): the vector from the bicipital groove (BG) and the humeral head center (HC); **V3** (verLT_HC): the vector from the lesser tubericle (LT) and HC; and **V4** (verLT_SA): the vector from LT and the shaft axis (SA). Note: V2 is not labeled for the right arm as it is nearly 0°. For this subject the measures of version (non-involved/involved) were as follows: **V1:** −10.3°/−48.2°, **V2:** 43.0°/0.1°, **V3:** 63.1°/24.0°, and **V4:** 79.5°/28.5°.

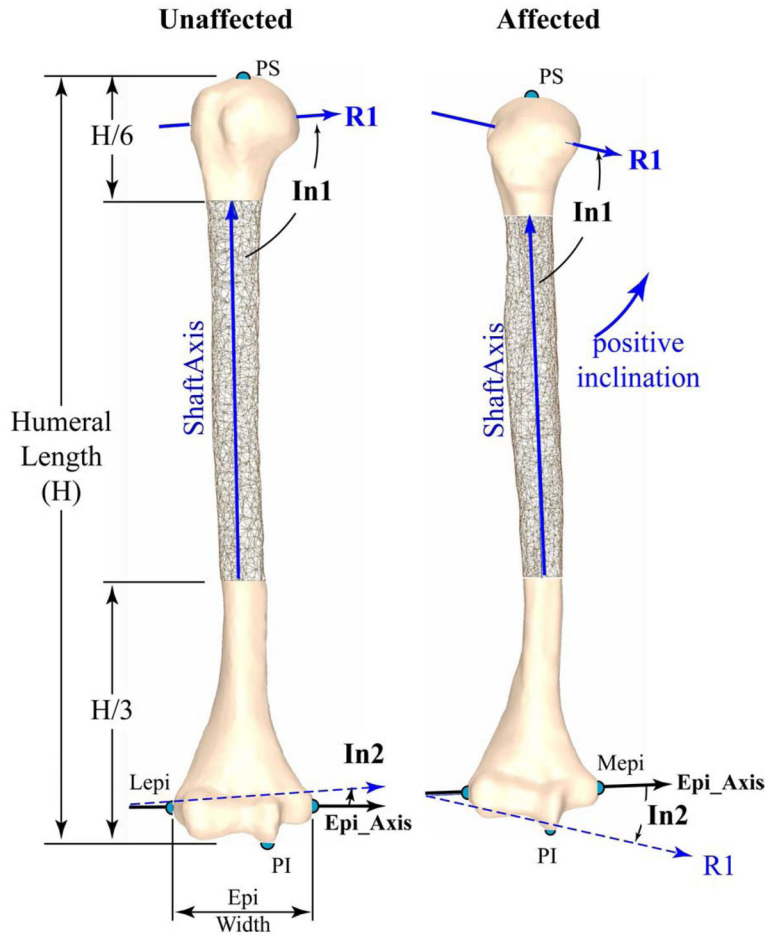

Figure 4. Inclination

The non-involved left (left) and involved right (right) humerii from a single subject (subject 8, the same as in Figure 3), as viewed in a pure coronal view (after humerii were aligned with the principal axes). A mirror image was created of the non-involved left arm (making it appear as a right arm) for direct visual comparison. Both images are scaled identically. **R1**, **R2**, and **R3** are the primary, secondary and tertiary radii of the best fit ellipsoid to the humeral head. **R1** is shown with an extended length. **R2** is in this coronal plane and perpendicular to **R1.** Both **R2** and **R3** are not shown for clarity. Inclination is positive when the medial humeral head rotates superiorly. Inclination was the angle between the first principal axis of the best fit ellipsoid to the humeral head (R1) and both the ShaftAxis (**In1:** head_incl_Shaft) and the epicondylar axis (**In2:** head_incl_Epi). Lepi and Mepi: most lateral and medial points of elbow epicondylar line; PS and PI: the most superior and inferior points of the humerus. For this subject the measures of inclination, H, and epi_width (non-involved/involved) were as follows: **In1:** 93.5°/75.7°, **In2:** 4.1°/−15.0°, **H**: 241.4 mm/327.4 mm; and **epi_width**: 63.5 mm/59.2 mm.

J Shoulder Elbow Surg. Author manuscript; available in PMC 2015 May 01.

Table 1

Comparison of version and inclination angles between sides

All measures are in degrees. For each measure, the average is provided with the standard deviation listed directly below in parentheses. The difference was relative to the non-involved side. Thus, the negative difference in inclination angle and version indicates that the medial head was declined and retroverted.

	Version				**Head Inclination**	
	R1	**BG_HC**	**LT_HC**	**LT_SA**	**Shaft Axis**	**Epicondylar Axis**
Involved side	−2.5 (28.2)	39.9 (33.0)	59.0 (32.9)	65.3 (37.1)	90.3 (7.9)	2.9 (10.7)
Non-involved Side	14.7 (12.6)	56.5 (9.4)	76.9 (12)	88.8 (13.4)	94.7 (6.5)	9.0 (8.1)
Paired difference between sides	**−17.2 (23.5)**	**−16.6 (26.3)**	**−17.9 (26.3)**	**−23.6 (31.1)**	**−4.4 (6.6)**	**−6.1 (7.6)**
Paired t-test	0.011	0.023	0.015	0.009	0.022	0.009

Note: for the inclination angle, the one subject that was deemed an outlier was removed. When this subject was removed from the version angles, there was little change in the average values of version and thus, their data remained in these averages. The p-values were derived using a one-tailed paired Student's t-test. This was followed by a false discovery rate Bonferroni correction. No p-values rose above 0.05 when a two-tailed test was used.

Table 2

Correlations between parameters for the non-involved arm

All r-values ≥0.45 are shown.

	head_incl_Epi	head_incl_Shaft	verR1	verBC_HC	verLT_HC	verLT_shaft
Age	**−0.71** 0.009			−0.50 0.085	−0.57 0.052	−0.55 0.062
R1	**−0.64** 0.026			−0.47 0.110	−0.53 0.079	**−0.62** 0.031
R2	**−0.65** 0.022			−0.51 0.075	−0.56 0.056	**−0.66** 0.021
R3	−0.5 0.097			−0.50 0.082	−0.56 0.060	**−0.65** 0.021
Humeral length	**−0.59** 0.044		−0.57 0.055	**−0.70** 0.008	**−0.68** 0.016	**−0.75** 0.005
Epicondylar Width	**−0.66** 0.02			**−0.58** **0.039**	**−0.58** 0.047	**−0.7** 0.011
head_incl_Epi	**NA**	**0.65** 0.023				
verR1			**NA**	**0.82** 0.001	**0.84** 0.001	**0.65** 0.022
verBC_HC				**NA**	**0.96** <0.001	**0.91** <0.001
verLT_HC					**NA**	**0.91** <0.001

The bolded text indicates a significant correlation ($p < 0.05$). NA: the correlation was not run.

Table 3

Correlations between the side-to-side differences in humeral morphological parameters

All r-values ≥0.45 are shown.

	head_incl_Epi	VerR1	VerBC_HC	VerLT_HC	VerLT_Shaft	Mallet	Narakas
Age		−0.45 0.122	−0.47 0.108				**NA**
R2		**−0.58** 0.037					
Humeral length						0.45 0.125	
Epicondylar Width	−0.562 0.057					0.76 0.003	
head_incl_Epi						−0.76 0.004	
head_incl_Shaft		0.45 0.146					
verR1		**NA**	0.61 0.026	0.69 0.010	0.61 0.027		−0.46 0.114
verBC_HC			**NA**	**0.98** <0.001	**0.98** <0.001		
verLT_HC				**NA**	**0.97** <0.001		

The bolded text indicates a significant correlation ($p < 0.05$). Passive range of external shoulder rotation is not shown as no correlation rose above r=0.45. NA indicates that the correlation was not run.

Table 4

Comparison of size between the involved and non-involved humeri

All measures are in mm, except the unit-less ratios (R1/R2, R1/R3, and R2/R3). For each measure, the average is provided with the standard deviation listed directly below in parentheses. R1, R2, and R3 (the primary, secondary, and tertiary radii of the best fit ellipsoid to the humeral head). R1, R2, and R3 were primarily in the medial-lateral direction, anterior-posterior, and inferior-superior direction. The difference was relative to the non-involved side. Thus, the negative difference in size measures indicates that the humerus on the involved side is smaller than on the non-involved side.

	R1	R2	R3	R1/R2	R2/R3	R1/R3	humeral length	Epicondylar width
Involved side	20.8 (3.4)	17.7 (3.2)	15.1 (3.0)	1.18 (0.05)	1.18 (0.12)	1.39 (0.12)	269.8 (41.1)	46.9 (11.0)
Non-involved Side	23.1 (3.5)	19.5 (3.3)	17.9 (3.2)	1.19 (0.04)	1.09 (0.04)	1.30 (0.07)	288.0 (42.0)	54.2 (9.9)
Paired difference between sides	**−2.3 (0.7)**	**−1.9 (1.0)**	**−2.8 (1.5)**	−0.01 (0.05)	**0.08 (0.10)**	**0.09 (0.12)**	**−18.2 (9.8)**	**−7.3 (4.7)**
Paired t-test	<0.001	<0.001	<0.001	0.335	0.005	0.010	<0.001	<0.001

Table 5

Inter-rater reliability

Analysis was based on 11 randomly selected humeri (6 from the involved side).

	ICC	Average absolute error between observers
R1	0.996	0.25 mm
R2	0.997	0.23 mm
R3	0.996	0.25 mm
Humeral Length	1.000	0.72 mm
Epicondylar Width	0.999	0.80 mm
head_incl_Shaft	0.984	1.64°
head_incl_Epi	0.960	2.84°
VerR1	0.973	3.31°

All ICCs had p-values <0.001. The variation between measures did not differ from the involved to the non-involved side.